



HAL
open science

Introducing 'trident': a graphical interface for discriminating groups using dental microwear texture analysis

Ghislain Thiery, Arthur Francisco, Margot Louail, Emilie Berlioz, Cécile Blondel, Noël Brunetière, Anusha Ramdarshan, Axelle Ec Walker, G Merceron

► To cite this version:

Ghislain Thiery, Arthur Francisco, Margot Louail, Emilie Berlioz, Cécile Blondel, et al.. Introducing 'trident': a graphical interface for discriminating groups using dental microwear texture analysis. 2023. hal-04222508

HAL Id: hal-04222508

<https://hal.science/hal-04222508>

Preprint submitted on 5 Oct 2023

HAL is a multi-disciplinary open access archive for the deposit and dissemination of scientific research documents, whether they are published or not. The documents may come from teaching and research institutions in France or abroad, or from public or private research centers.

L'archive ouverte pluridisciplinaire **HAL**, est destinée au dépôt et à la diffusion de documents scientifiques de niveau recherche, publiés ou non, émanant des établissements d'enseignement et de recherche français ou étrangers, des laboratoires publics ou privés.

1 **Introducing ‘trident’: a graphical interface**
2 **for discriminating groups using dental**
3 **microwear texture analysis**
4

5 Thiery G.^{1,2}, Francisco A.³, Louail M.¹, Berlioz E.^{1,4}, Blondel C.¹, Brunetière N.³, Ramdarshan
6 A.¹, Walker A. E. C.¹, Merceron G.¹
7

- 8 1. Laboratoire PALEVOPRIM, UMR 7262, CNRS & Université de Poitiers, France
9 2. Center for Evolutionary Origins of Human Behavior EHUB, Kyoto University Museum,
10 Japan
11 3. Institut Pprime, UPR CNRS 3346, Université de Poitiers, France
12 4. EvoAdapta Group, University of Cantabria, Santander, Spain
13
14
15

16 Corresponding authors: A. Francisco, G. Merceron

17 gildas.merceron@univ-poitiers.fr

18 arthur.francisco@univ-poitiers.fr
19

20 **Abstract**

21

22 This manuscript introduces trident, an R package for performing dental microwear texture
23 analysis and subsequently classifying variables based on their ability to separate discrete
24 categories. The trident package comes with independent functions and a user interface,
25 trident, enabling easy and fast proficiency. It can import .SUR files, then remove aberrant
26 peaks and possibly polynomial surfaces in the 2nd or 8th order. Next, it can measure up to 384
27 variables corresponding to 24 parameters and their heterogeneity. It can also rank any
28 number of variables using five different methods, display the results in multivariate analyses,
29 and export the results in R, providing access to its large asset of libraries.

30 We then present these features in three case studies, showing how trident helps answer
31 questions commonly investigated by paleontologists and archaeologists. In the first case
32 study, we separate four groups of domestic pigs based on their dietary composition. In the
33 second case study, we identify microwear texture patterns in a large database of 15 primate
34 species and relate these patterns to biomechanical and ecological factors. The third case
35 study investigates the dental microwear textures of four extant ruminants to infer the diet of an
36 extinct antelope from the Pleistocene of Greece. These case studies show how trident can
37 leverage dental microwear texture analysis results.

38

39 Keywords: Diet inference; DMTA; Multivariate analysis

40 **Introduction**

41 **Fifty shades of dental microwear**

42 Dental microwear analysis has been a prominent method for investigating the diet of extant
43 and extinct species during the last 40 years (e.g., Walker et al., 1978; Kay, 1981; Teaford,
44 1985, 1988; Ungar, 1996; Teaford et al., 1996; Solounias & Semprebon, 2002; Merceron et al.,
45 2005; Merceron, Blondel, et al., 2005; Scott et al., 2005; Ungar et al., 2008; Rivals et al. 2011).
46 It is based on the observation that food leaves microscopic wear marks on dental wear facets,
47 and that those marks fade as the tooth wears, only to be replaced by new microwear marks
48 (Walker et al., 1978; Gordon, 1982; Teaford & Oyen, 1989; Winkler et al., 2020). The nature
49 (scratches or pits), size (small to large), and frequency of microwear depend on the food's
50 physical properties, mostly hardness, and abrasiveness, while their spatial distribution and
51 their anisotropy are related to chewing motions and food toughness (Teaford, 1988; Scott et
52 al., 2006; Teaford et al., 2020). This allows us to infer an animal's diet during the last few
53 weeks before its latest meal (Teaford & Oyen, 1989; Winkler et al., 2020). Apart from diet, the
54 role of exogenous soil mineral particles and environmental conditions in dental microwear
55 formation should not be minimized (Schulz-Kornas et al., 2019; Schulz-Kornas et al., 2020).
56 Grit is indeed reportedly harder than enamel tissue and more abrasive than food particles
57 (Sanson et al., 2007; Lucas et al., 2013). Still, controlled feeding experiments have shown
58 that differences in dental microwear texture better reflect diet than the amount of exogenous
59 particles (Merceron et al., 2016).

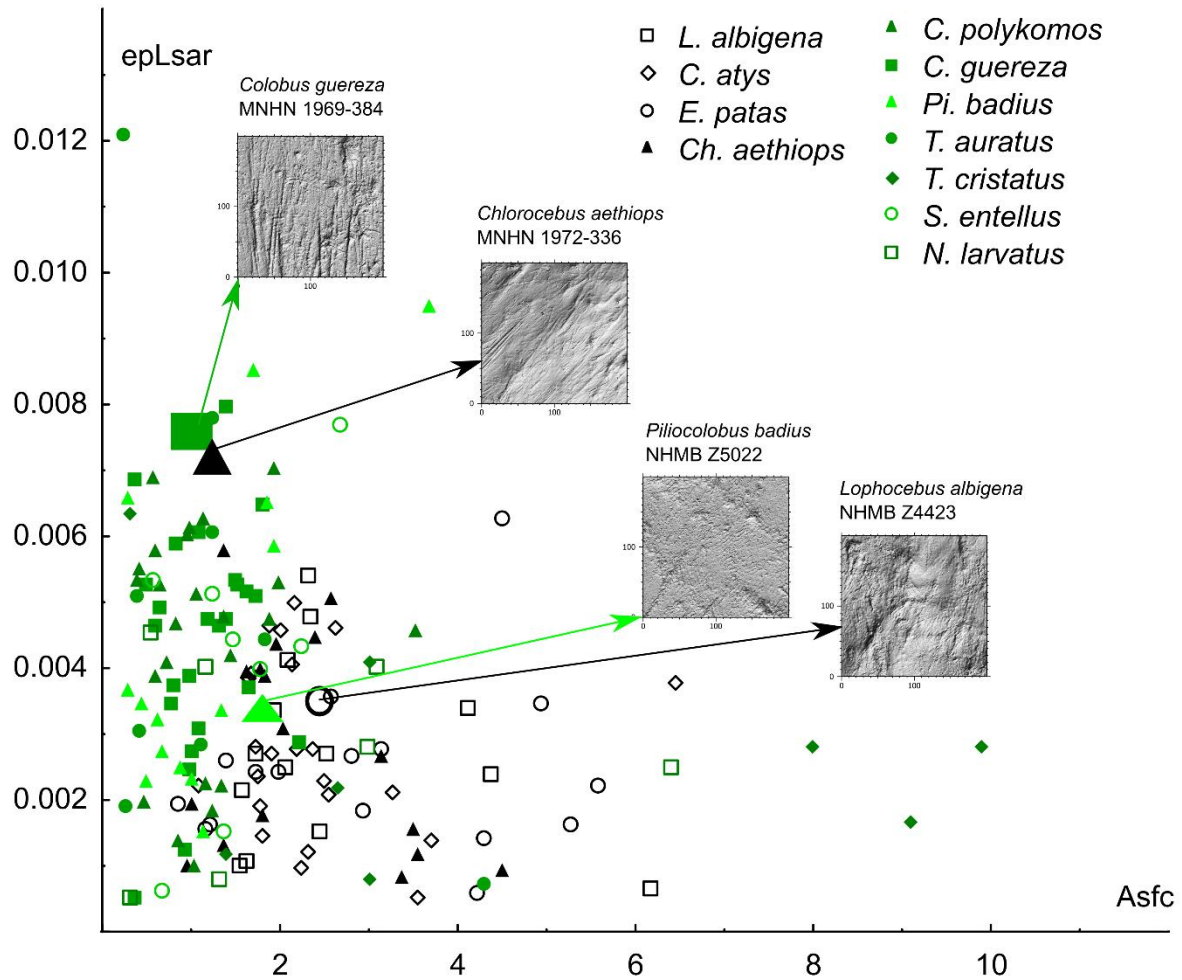
60 Initially, microwear analysis used light microscopes to count pits and scratches left by the food
61 on the enamel surface. But despite a proven ability to separate surfaces according to diet, this
62 method is reliant on the tuning of light orientation, the counting method, the observer
63 experience, etc. (Grine et al., 2002; Galbany et al., 2005; Muhlbachler et al., 2012). With the
64 advent of high-resolution digitization techniques, new methods for quantifying the three-

65 dimensional surface texture have emerged. Scale Sensitive Fractal Analysis (SSFA) uses
66 surface parameters strongly correlated to food material properties, such as surface scale
67 roughness estimated from area-scale fractal complexity (Asfc) that correlates to food
68 hardness, or anisotropy (epLsar) that correlates to food toughness (Ungar et al., 2003; Scott
69 et al., 2005; Hua et al., 2020). A second approach, Surface Texture Analysis (STA) consists of
70 computing ISO-25178 area parameters (Schulz et al., 2010; Kaiser et al., 2015). Both SSFA
71 and STA methods belong to the larger field of dental microwear texture analysis (DMTA).
72 They have been used to investigate the diet of animals from a broad range of species,
73 including insectivorous mammals (Purnell et al., 2013) but also selacians (Weber et al., 2021),
74 lepidosaurians (Winkler et al., 2019) or dinosaurs (Williams et al., 2009).

75 **New methods, new challenges**

76 Despite their reliability, DMTA approaches are facing several methodological challenges. First,
77 they sometimes fail to separate specimens that an expert eye could visually tell apart using
78 the number of specific microwear marks (Fig. 1). This can be mitigated by using filters to
79 enhance the microwear versus the raw shape of the tooth surface, for instance by removing
80 the 2nd or 8th order polynomial of the surface using least square approximation (Francisco,
81 Brunetière, et al., 2018). Failure to tell surfaces apart can also come from distinct structures
82 concealed in the average signal. One of the SSFA parameters can solve this issue by
83 estimating heterogeneity of complexity (HAsfc, Scott et al., 2005, 2006). An alternative
84 approach is to consider a grid of standard number and size of cells and to measure every
85 parameter for each cell: the presence of distinct structures would increase the dispersion of
86 values, and could be detected using percentiles, minimal or maximal values, etc. (Francisco,
87 Blondel, et al., 2018).

88



89

90 Figure 1. Cases where an expert eye can visually differentiate two surfaces, but dental microwear texture
 91 analysis cannot. For example, experts will count more wide scratches on *Colobus guereza* (MNHN 1969-384)
 92 compared to *Chlorocebus aethiops* (MNHN 1972-336) whereas DMTA fails to discriminate the two using both
 93 anisotropy and complexity. Similarly, experts will count more large pits on *Lophocebus albigena* (NHMB Z4423)
 94 compared to *Piliocolobus badius* (NHMB Z5022) whereas DMTA fails to discriminate the two. In the latter
 95 example, we expect heterogeneity to solve the issue.
 96

97 Computing heterogeneity of DMTA variables helps track the most elusive structures, but it
 98 tends to generate a “jungle of parameters” (Francisco, Brunetière, et al., 2018), that is, too
 99 many variables to keep track of a given phenomenon. One way to bypass this issue is to
 100 compare the variables’ ability to discriminate groups, for instance using analyses of variance
 101 (ANOVAs) to find which groups can be separated using post-hoc analysis such as Tukey’s
 102 HSD or Fisher’s LSD. This analysis pipeline is very efficient and could separate animals

103 according to their diet in several studies (Francisco, Blondel, et al., 2018; Francisco,
104 Brunetière, et al., 2018; Louail et al., 2021; Merceron, Kallend, et al., 2021).

105 Yet two more limitations can be identified. The first one concerns the repeatability of
106 measures, as the code was not accessible in previous works. The second limitation is the
107 ease of use since the pipeline made use of a combination of Fortran, Python, and R to collect
108 the data. Consequently, fine-tuning the nature of data collection and analysis was only
109 possible for people familiar with those languages. An open-source user interface would solve
110 both issues and make measuring, analyzing, and untangling DMTA data easier, faster, and a
111 lot more intuitive for beginners.

112 Here, we introduce trident, a user interface, and its associated R source package trident for
113 measuring dental microwear textures and analyzing the discriminant ability of DMTA variables.
114 It can load .SUR files, remove abnormal peaks, and measure 16 variables from 24 DMTA
115 parameters (for a total of 384 variables) on batches. The computed DMTA variables (along
116 with variables possibly added by the user on the source .txt file) can be classified according to
117 their ability to discriminate discrete categories such as species, diet, etc trident also comes
118 with tools to perform univariate, bivariate, and multivariate analysis. All the functions can be
119 performed from the user interface.

120 We then showcase its functionalities using three case studies, representative of research
121 questions that could be answered using dental microwear analysis:

122 Case study A. Diet-related differences in dental microwear: The first case study is based
123 on a controlled feeding experiment involving a single omnivorous species (*Sus*
124 *domesticus*). Similar to Louail et al. (2021), animals participated in trials only differing
125 in the dietary composition of their daily ration. The influence of diet on DMTA was then
126 quantified using trident.

127 Case study B. Meta-analysis of a large multi-species sample: The second case study is
128 based on a large sample grouping 260 specimens from 15 species of cercopithecoid
129 primates of Asia and Africa. We used trident to detect patterns related to species, their
130 tribe (Cercopithecini, Colobini, Papionini, and Presbytini), or their general diet
131 according to the literature.

132 Case study C. Comparison with extant species to infer the diet of extinct species: The
133 third case study is based on four sympatric species of ruminants from the Bauges
134 Natural Regional Park, French Alps. In a previous study, SSFA variables could find
135 differences between species, reflecting differences in dietary behavior and spatial use
136 (Merceron, Berlioz, et al., 2021). We used trident to explore the dental microwear
137 textures of this community and then used the most discriminating variables to make
138 inferences on the diet of *Gazellospira torticornis*, an extinct antelope from Greece
139 (Hermier et al., 2020).

140 **Material and Methods**

141 **Material**

142 ***Case study A: Diet-related differences in dental microwear***

143 The first case study is based on three of the feeding trials with domestic pigs (*Sus domesticus*)
144 detailed in Louail et al. (2021), to which was added another trial. The control group (N = 5)
145 was fed exclusively with a base diet composed of ground cereal and soy seeds. The three
146 other groups were also fed this base diet, with a supplement depending on their group:

- 147 • The *barley group* (N = 5) was fed 30 % of barley seeds.
- 148 • The *corn kernel group* (N = 5) was 20 % of corn (*Zea mays*) flour, supplemented with
149 20 % (as dry matter weight) of corn kernels.
- 150 • The *corn silage group* (N = 5) was fed 100 % of the base diet but had access to corn
151 silage at will.

152 We analyzed the deciduous upper fourth premolars of pigs aged between 6.5 and 9.5 months.
153 For more details on the experiment, see Louail et al. (2021).

154 ***Case study B: Meta-analysis of a large multi-species sample***

155 The second case study is based on skulls and jaws of extant cercopithecids from osteological
156 collections of Europe, Asia, and Africa (for a detailed listing of institutions, see Supplementary
157 Materials 1). A total of 260 casts of upper and lower second molars from 15 extant species
158 were obtained as detailed in previous studies (Merceron, Kallend, et al., 2021; Thiery et al.,
159 2021). Each tribe of extant cercopithecids (Cercopithecini, Colobini, Papionini, and Presbytini)
160 is represented by at least 2 species (Supplementary Materials 1). Overall, the selected taxa
161 encompass a broad range of diets, from a large geographic range (see Rowe et al., 1996 and
162 citations therein).

163 **Case study 3: Comparison with extant species to infer the diet of extinct species**

164 The Bauges Natural Regional Park is a typical subalpine massif located in the French Alps. In
165 the third case study, four extant ruminants from the Bauges have been investigated: *Cervus*
166 *elaphus*, a mixed-feeding species; *Capreolus capreolus*, a selective browser; *Ovis gmelini*
167 *musimon*, and *Rupicapra rupicapra*, two bovid species known to be mixed feeders. Mandibles
168 were collected at the same locality, during a short period (for more details, see Merceron,
169 Berlioz, et al., 2021), representing a hypothetical fossil assemblage composed of different
170 species occupying different small-scale habitats (open alpine grassland, bushland, shrubland,
171 deciduous, mixed, coniferous forests) in a common geographical range.

172 These four extant species were then compared to the extinct antelope *Gazellospira torticornis*
173 (Bovidae), from the Early Pleistocene of Greece. Specimens come from the site of Dafnero
174 and have been described by Hermier et al. (2020).

175 **Surface acquisition**

176 Each tooth surface was cleaned and molded as described in previous works (Louail et al.,
177 2021; Merceron, Berlioz, et al., 2021; Merceron, Kallend, et al., 2021) and on the TRIDENT
178 website (<http://anr-trident.prd.fr/v/>). For case study A, we investigated both the shearing
179 (phase I) and crushing (phase II) dental facet of the very same tooth, whereas we focused on
180 crushing facets for case study B (primates) and on shearing facets for case study C
181 (ruminants). Each facet was scanned separately using a white-light confocal profilometer
182 Leica DCM8, named “TRIDENT”, with a 100× objective housed at the PALEVOPRIM lab,
183 CNRS and University of Poitiers, France (Leica Microsystems). All surfaces were pre-
184 processed following Merceron et al. (2016). The procedure resulted in the obtention of .SUR
185 files (saved as SUR version 7.2 or older), which were then imported into trident.

186 **DMTA with *trident***

187 ***Presentation of trident***

188 Here we introduce the R source package *trident*, which is devoted to measuring microwear
189 textures and classifying variables according to their discriminant power. It was implemented
190 on two levels:

191 (1) Functions that can be launched from the R console, for which detailed instructions can
192 be found in the metadata and the help files of the package.

193 (2) A shiny app named *trident*, which is launched from the console using the line
194 `trident.app()`. The app is a wrapper for the package functions, connecting them to
195 other packages for statistical analyses, multivariate analyses, or graphical rendering.

196 Below are summarized the functionalities of the interface used in the three case studies. The
197 reader can find a more detailed description of the interface in the user manual, provided as
198 supplementary materials (Supplementary Materials 2).

199 ***Dental microwear texture analysis (DMTA)***

200 Surfaces were first enhanced using the polynomial removal procedure; all procedures
201 mentioned below are detailed in Francisco, Brunetière et al. (2018). The primary surface S1
202 was first numerically and automatically cleaned of any abnormal peaks. Then, considering the
203 large-scale tooth surface geometry as an 8th-order polynomial (PS8), the latter was
204 subtracted via a least square approximation. This procedure was performed on surfaces of
205 the same size, as subtracting PS8 from smaller surfaces would remove larger amounts of
206 relief. The software also allows to remove of the 2nd order polynomial (PS2).

207 Afterward, DMTA variables were computed. The program can currently compute four families
208 of parameters (Table 1). The first one is complexity i.e., an estimation of the density of
209 microwear textures. The second family is height, or parameters describing the average height,
210 its dispersion, and its variation over the surface. The third family is spatial parameters, which

211 describe the distribution and nature of the textures. The last family is topology, a combination
 212 of height and spatial parameters, measuring the proportion of the surface above or below
 213 determined heights.

214 Table 1. DMTA parameters measured in trident

Parameter	Family	Significance
Asfc2	Complexity	Area scale fractal complexity([#])
Sa	Height	Arithmetic mean of the absolute of the heights (*)
Sp	Height	Absolute of the largest height (*)
Sq	Height	Height standard deviation (*)
Sv	Height	Absolute of the smallest height (*)
Ssk	Height	Height skewness (*)
Sku	Height	Height kurtosis (*)
Sm	Height	Mean height (0 for the whole surface, but non-zero for its samples)
Smd	Height	Median height
Rmax	Spatial	Semi-major axis of the fACF ellipsis(**)
Sal	Spatial	Semi-minor axis of the fACF ellipsis (**)
Std ^{EX}	Spatial	Texture direction (**)
Stri(*) = Str ⁻¹	Spatial	Rmax/Sal ratio
b.sl	Spatial	Highest slope of fACF (**) at the distance rs from the origin
r.sl	Spatial	b.sl/s.sl ratio
s.sl	Spatial	Smallest slope of fACF (**) at the distance rs ^β from the origin
Sdar	Complexity	Relative area (developed area/projected area)
Sk1, Sk2	Topology	Relative area of the surface above h1 ^{ββ} and h2 ^{ββ} respectively
Smc1, Smc2	Topology	Median relative area of the cells with heights exceeding h1 ^{ββ} and h2 ^{ββ} respectively
Snb1, Snb2	Topology	Number of cells with heights exceeding h1 ^{ββ} and h2 ^{ββ} respectively
Sh	Topology	Percentage of quasi-horizontal faces (normal within a 4° cone)

215 ^{EX}, parameters excluded from the analysis; * ISO 25178 ; ** autocorrelation function at z=0.5 (Francisco, Blondel,
 216 et al., 2018; Francisco, Brunetière, et al., 2018) ; ^β maximum slope radius ; ^{ββ} h1 = 85 % of total height (Sv+Sp)
 217 and h2 = 95 % of total height (Sv+Sp)[#] ; Area Scale Fractal Complexity is labeled Asfc2 because its calculation
 218 mode slightly differs from the Asfc computed in Scott et al., 2006).
 219

220 Lastly, we estimated the heterogeneity for complexity, height, spatial, and topology variables.
 221 The heterogeneity of a (dental) surface is related to the spatial distribution of its features: for
 222 instance, a single pit in the enamel implies more heterogeneity than several pits uniformly
 223 distributed through the enamel surface (Scott et al., 2006). Following Francisco, Brunetière et

224 al. (2018), trident uses a fast and intuitive approach for estimating heterogeneity: the surface
225 is divided into n grid cells, and DMTA parameters are computed for each grid cell. Then, the
226 distribution of DMTA parameters across grid cells is used to compute heterogeneity variables
227 e.g., mean Asfc2, maximal Asfc2, or 25th percentile of Asfc2 (Table 2). Note that this way of
228 assessing heterogeneity differs from SSFA parameters such as HAsfc (Box 1). In the end, a
229 total of 384 variables can be computed, giving a highly detailed description of dental
230 microwear textures. Out of these, 24 variables correspond to the 24 parameters from Table 1
231 measured on the whole surface, but the remaining 360 are estimates of surface heterogeneity.

232 Box 1. trident and the traditional SSFA variables

233 trident does not allow to compute of SSFA variables. Still, the user can find equivalents among the 384
234 variables available in trident. For instance, Asfc can be approximated from Asfc2, which also strongly
235 correlates with Sdar. EpLsar, which is an SSFA estimate of anisotropy, is related to spatial variables in
236 trident. It is especially correlated with Rmax, Sal, and Stri (Str^{-1}). Note that trident can open and manage
237 any other variables (e.g., SSFA, furrows, $\delta^{13}\text{C}$...) that a user might want to add to the source .txt file.
238 This way, it is easy to compare trident's variables with other parameters.

239

240 In each of the three case studies, all variables except minimal and maximal values were
241 calculated on 23 parameters (Std was excluded because it is scanning orientation-
242 dependent), for a total of 322 variables: this avoids measuring the effect of a single feature. To
243 assess the heterogeneity, the resampling statistics were calculated for a grid of 256 cells
244 (16×16).

245 Table 2. Heterogeneity variables.

Statistics	Description
min ^{EX}	Minimal value
max ^{EX}	Maximal value
sd	Standard deviation
mean	Arithmetic mean
med	Median
fst.05	5 th percentile
lst.05	95 th percentile
min.05	Mean of values under the 5 th percentile
max.05	Mean of values above the 95 th percentile
fst.25	1 st quartile
lst.25	3 rd quartile
min.25	Mean of values under the 1 st quartile
max.25	Mean of values above the 3 rd quartile
skw	Skewness of the histogram of distribution
kurt	Kurtosis of the histogram of the distribution

246 ^{EX}, variables excluded from the analysis.

247 **Multichecks**

248 The second most important part of trident relates to the classification of variables according to
 249 their ability to separate informed categories, such as diet, species, etc. In case study A, the
 250 factor is diet whereas in case study B and C, the factor is species. The software proposes
 251 functions for adding a factor variable by combining variables from different datasets, by
 252 entering it manually or automatically (see Supplementary Materials 2).

253 Afterward, the discriminant ability of variables is calculated using a pipeline of analysis initially
254 designed by Francisco and colleagues (Francisco, Blondel, et al., 2018; Francisco, Brunetière,
255 et al., 2018):

256 (a) Normality: the normality of the data is tested using the Shapiro-Wilk test. If
257 unsuccessful, we compute the skewness ratio, computed as the skewness divided by
258 its confidence interval. If the skewness ratio is inferior to 2, the distribution is
259 considered nearly normal.

260 (b) Homoscedasticity: for normally distributed data, the homogeneity of variances is tested
261 using the Bartlett test. If the test fails, the groups are still nearly homoscedastic if the
262 variance ratio, computed as the maximum variance divided by the minimum variance
263 for each group, is lower than 3. For nearly normal data, Levene's test is performed to
264 check the group variance homogeneity.

265 (c) Ability to separate categories: If both normality and homoscedasticity assumptions are
266 respected, or if no more than one condition is nearly respected, then the discriminant
267 ability of variables is tested using an ANOVA. Otherwise, the discriminant ability of
268 variables is tested using a non-parametric test, the Kruskal-Wallis test.

269 All these tests are implemented with a default alpha of 0.05. They have been grouped in a
270 'multi check' function (Supplementary Materials 2). If data are not normally distributed, they
271 can also be transformed using either a base 10 logarithm function or a Box-Cox
272 transformation (Supplementary Materials 2).

273 ***Classification of variables***

274 We implemented five different classification methods, which can be used depending on the
275 situation:

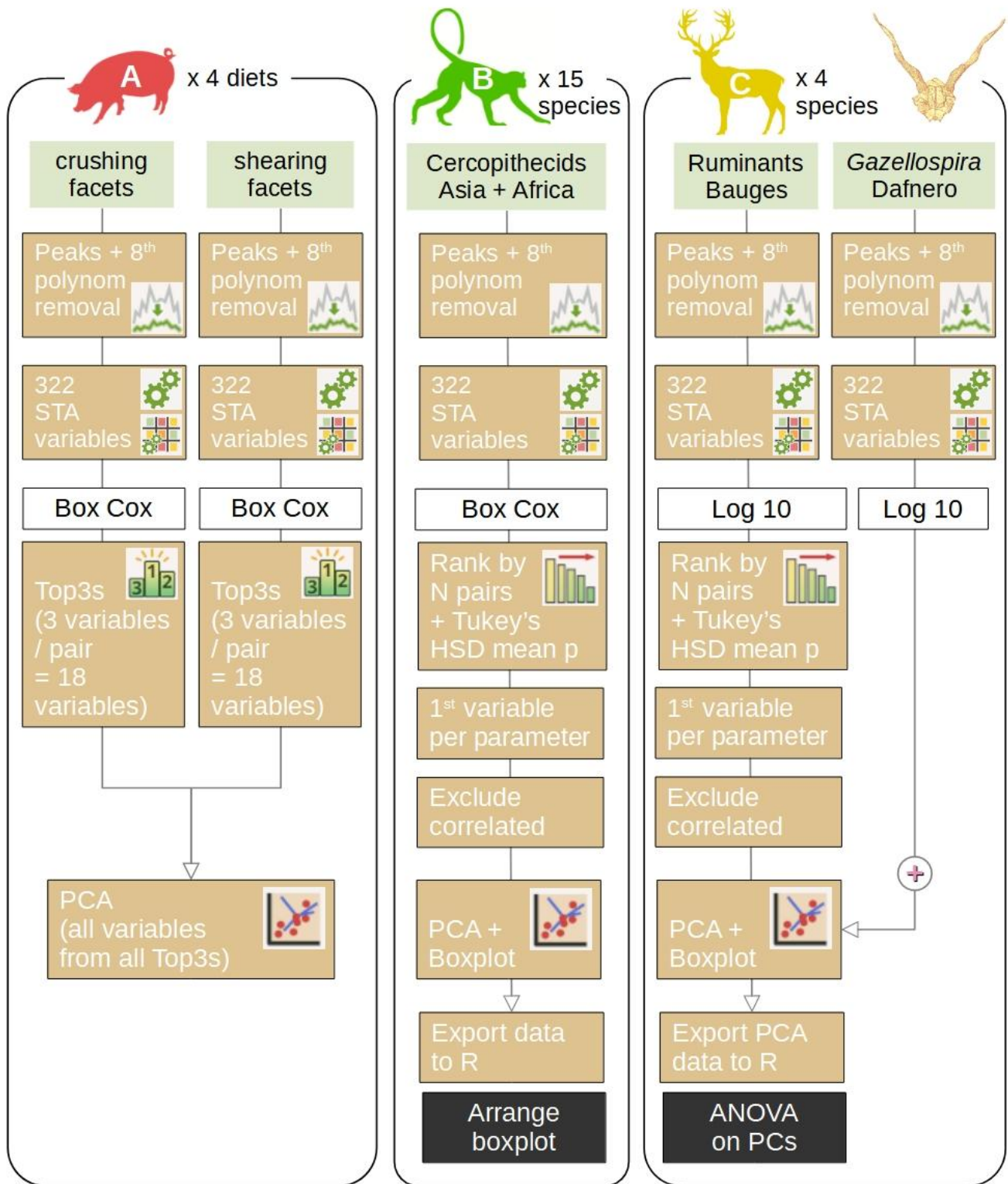
276 (1) Rank based on ANOVA: Performs an ANOVA and arranges variables by ascending p-
277 value.

- 278 (2) Rank based on Kruskal-Wallis: Performs a Kruskal-Wallis rank-sum test and arranges
279 variables by ascending p-value; in case the sample is far from normality.
- 280 (3) Rank based on post-hoc (average): Performs an ANOVA and arranges by decreasing
281 the number of significant p-values per pair and then ascending mean p-value from
282 post-hoc tests. The mean p-value can be either arithmetic or geometric, and the user
283 can choose to use only significant p-values to calculate it (this is the default option).
- 284 (4) Rank based on post-hoc (pairwise): Performs an ANOVA and then for a given pair,
285 arranges variables by ascending pairwise post-hoc p-value.
- 286 (5) Top 3: For each pair of categories, arrange by the number of significant pairwise p-
287 values from Tukey's HSD, then by the mean of significant p-values. The function
288 returns the 3 best-classified variables. Because this function makes a new
289 classification for each pair of groups, computation time and length of results increase
290 exponentially as the number of categories goes up. Although it remains possible to use
291 this function on any number of categories, we do not recommend using this approach
292 for more than 5 categories (10 pairs).

293 Note that all these tests are implemented with a default alpha of 0.05. Regardless of the
294 chosen workflow, it is possible to visualize variables using boxplots and violin plots. It is also
295 possible to perform a principal component analysis (PCA) on a selection of variables. It
296 provides a histogram of the percentage of variance explained by each principal component
297 (screenplot), as well as buttons for saving and exporting the PCA results, a bivariate diagram
298 of the selected principal components, and circles of correlations. Graphics can be saved as
299 images.

300 **Case-specific analysis**

301



302
303 Figure 2. Flowchart depicting the analysis for the three case studies.

304 **Case study A: Diet-related differences in dental microwear**

305 For each wear facet (crushing and shearing), data were analyzed separately. They were Box-
306 Cox transformed, then checked for normality, homoscedasticity, and their ability to

307 discriminate categories (Fig. 2A). Variables that passed the multi check were classified using
308 the mean of the significant p-values from Tukey's HSD post-hoc analysis of an ANOVA with
309 diet as factor. They were ranked according to (1) the number of groups discriminated and (2)
310 the arithmetic mean of Tukey's HSD discriminant p-values (the p-value of non-discriminated
311 groups were ignored for calculating this arithmetic mean). Among these variables, we retained
312 only the 3 best-ranked variables (Top3). Afterward, all the retained variables for both crushing
313 and shearing facets were combined. We performed a Principal Component Analysis (PCA) to
314 explore their influence on data distribution. All analyses were done exclusively in trident.

315 ***Case study B: Meta-analysis of a large multi-species sample***

316 Data were Box-Cox transformed, then checked for normality, homoscedasticity, and their
317 ability to discriminate categories (Fig. 2B). Variables that passed the checking step were
318 classified using the results of a post-hoc analysis of an ANOVA with species as a factor. They
319 were ranked according to (1) the number of groups discriminated and (2) the geometric mean
320 of Tukey's HSD discriminant p-values (the p-value of non-discriminated groups were ignored
321 for calculating this geometric mean). Then, for each parameter (e.g., Asfc2), the best-ranked
322 variable out of 14 (central + heterogeneity statistics, see Table 2) was selected. Afterward, we
323 selected parameters with a correlation of Pearson below 0.70: variables correlated to more
324 than 70 % with a better-ranked variable were systematically removed (calculated
325 independently with R). The remaining variables were used for a PCA. All analyses were done
326 in trident, but the boxplots of the first two principal components were modified for the
327 purposes of this article in R using the ggplot2 package (Wickham et al., 2021).

328 ***Case study C: Comparison with extant species to infer the diet of extinct species***

329 First, the Bauges data were log-transformed (base 10), then checked for normality,
330 homoscedasticity and their ability to discriminate species (Fig. 2C). Variables which passed

331 the checking step were classified using (1) the number of groups discriminated by the post-
332 hoc analysis of an ANOVA and (2) the geometric mean of Tukey's HSD discriminant p-values
333 (the p-value of non-discriminated groups were ignored for calculating this geometric mean).
334 Just like case study B, for each parameter (e.g., Asfc2), the best ranked variable out of 14
335 (central + heterogeneity statistics) was selected, and variables correlated to more than 70 %
336 with a better ranked variable were systematically removed (calculated independently with R).
337 The remaining variables were used for a PCA. At this point, the surfaces of *Gazellospira*
338 *torticornis* were added as supplementary individuals to the PCA. All analyses were done in
339 trident, but the boxplots of the first two principal components were modified in R using the
340 ggplot2 package. Afterwards, the principal components were exported to R and used for an
341 analysis of variance (ANOVA). The post-hoc analysis was performed using Tukey's HSD test.

342 **Results**

343 **Case study A: Diet-related differences in dental microwear**

344 The first analysis, a top-3 classification performed on crushing facets after Box-Cox
345 transformation (Table 3), revealed that the most discriminant variables are central height
346 skewness (Ssk), central topology variables (Sk1, Sk2, Smc1, Snb1) and heterogeneity
347 variables for complexity (Asfc2), height (Sq, Sv, Smd) and topology parameters (Sh). In
348 contrast, the same analysis performed on shearing facets (Table 4) revealed that the most
349 discriminating variables are central height kurtosis (Sku), the standard deviation of central
350 height skewness (Ssk.sd), mean and median of Smd, as well as skewness and kurtosis of
351 spatial variables (Sal, r.sl). There are no common variables between the top 3 of crushing and
352 shearing facets.

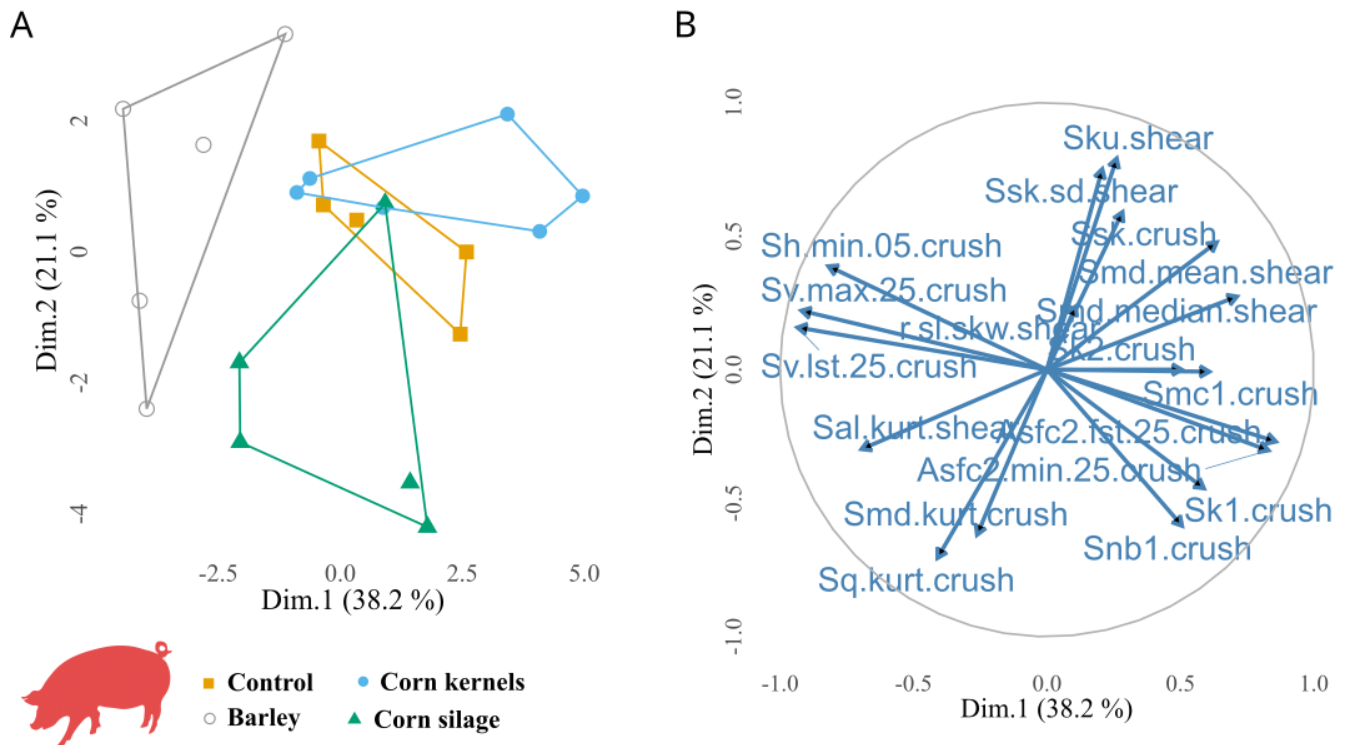
353 When combining the most discriminating variables from both crushing and shearing facets in
354 a principal component analysis (Fig. 3), the first and second PCs explain 38.2 % and 21.1 %
355 of the variances, respectively. Along PC1 and PC2, the control category overlaps with corn
356 kernels and corn silage categories, but other groups are distinctly separated (Fig. 3A). In fact,
357 PC1 separates barley-fed pigs from other categories, whereas PC2 separates seed-fed pigs
358 (barley and corn) from silage-fed pigs. Other PCs failed to separate categories and were not
359 pictured, but are available as supplementary materials (Supplementary Materials 1).

360 Table 3. Case study A: Diet-related differences in dental microwear, pairwise top 3 variables for the crushing
 361 facets. All variables Box-Cox transformed. Ba, barley; Co, control; CK, corn kernel; CS, corn silage.

pair <i>i</i>	TOP3 variables for the pair <i>i</i>	rank	<i>F</i>	<i>p</i> value ANOVA	Post hoc <i>p</i> values					
					Ba-Co	Ba-CK	Ba-CS	Co-CK	Co-CS	CK-CS
Ba-Co	Snb1	1	9.02	<0.01	0.09	0.10	0.02	1.00	0.89	0.80
	Asfc2.fst.25	2	5.58	0.02	0.09	0.06	0.09	1.00	1.00	1.00
	Sh.min.05	3	3.69	0.06	0.10	0.06	0.07	1.00	1.00	1.00
Ba-CK	Sv.lst.25	1	4.47	0.03	0.15	0.03	0.20	0.84	1.00	0.77
	Sv.max.25	2	4.83	0.03	0.15	0.04	0.18	0.93	1.00	0.89
	Smc1	3	6.88	0.01	0.42	0.04	0.23	0.58	0.97	0.83
Ba-CS	Snb1	1	9.02	<0.01	0.09	0.10	0.02	1.00	0.89	0.80
	Sk1	2	8.33	0.01	0.20	0.08	0.07	0.97	0.93	1.00
	Asfc2.min.25	3	4.69	0.03	0.13	0.07	0.07	0.99	0.99	1.00
Co-CK	Smd.kurt	1	4.82	0.03	1.00	0.18	0.66	0.26	0.54	0.02
	Sk2	2	4.58	0.04	0.80	0.08	0.84	0.39	1.00	0.35
	Ssk	3	5.45	0.02	0.51	1.00	0.84	0.57	0.15	0.74
Co-CS	Ssk	1	5.45	0.02	0.51	1.00	0.84	0.57	0.15	0.74
	Sq.kurt	2	5.21	0.03	0.92	0.33	0.81	0.70	0.45	0.07
	Smd.kurt	3	4.82	0.03	1.00	0.18	0.66	0.26	0.54	0.02
CK-CS	Smd.kurt	1	4.82	0.03	1.00	0.18	0.66	0.26	0.54	0.02
	Sq.kurt	2	5.21	0.03	0.92	0.33	0.81	0.70	0.45	0.07
	Sk2	3	4.58	0.04	0.80	0.08	0.84	0.39	1.00	0.35

362 Table 4. Case study A: Diet-related differences in dental microwear, pairwise top 3 variables for the shearing
 363 facets. All variables Box-Cox transformed. Ba, barley; Co, control; CK, corn kernel; CS, corn silage.

pair <i>i</i>	TOP3 variables for the pair <i>i</i>	rank	<i>F</i>	<i>p</i> value ANOVA	Post hoc <i>p</i> values					
					Ba-Co	Ba-CK	Ba-CS	Co-CK	Co-CS	CK-CS
Ba-Co	Sal.kurt	1	3.68	0.06	0.01	0.06	0.33	0.70	0.24	0.78
	r.sl.skew	2	5.49	0.02	0.28	0.98	0.17	0.12	0.99	0.07
	Smd.mean	3	5.18	0.03	0.28	0.05	0.98	0.81	0.46	0.10
Ba-CK	Smd.mean	1	5.18	0.03	0.28	0.05	0.98	0.81	0.46	0.10
	Sal.kurt	2	3.68	0.06	0.01	0.06	0.33	0.70	0.24	0.78
	Smd.median	3	5.76	0.02	0.35	0.07	0.59	0.79	0.97	0.53
Ba-CS	r.sl.kurt	1	5.68	0.02	0.33	0.95	0.11	0.13	0.90	0.03
	Skv	2	3.85	0.05	0.86	0.85	0.13	1.00	0.03	0.02
	r.sl.skew	3	5.49	0.02	0.28	0.98	0.17	0.12	0.99	0.07
Co-CK	r.sl.skew	1	5.49	0.02	0.28	0.98	0.17	0.12	0.99	0.07
	r.sl.kurt	2	5.68	0.02	0.33	0.95	0.11	0.13	0.90	0.03
	Ssk.sd	3	6.01	0.02	1.00	0.69	0.30	0.62	0.36	0.04
Co-CS	Skv	1	3.85	0.05	0.86	0.85	0.13	1.00	0.03	0.02
	Sal.kurt	2	3.68	0.06	0.01	0.06	0.33	0.70	0.24	0.78
	Ssk.sd	3	6.01	0.02	1.00	0.69	0.30	0.62	0.36	0.04
CK-CS	Skv	1	3.85	0.05	0.86	0.85	0.13	1.00	0.03	0.02
	r.sl.kurt	2	5.68	0.02	0.33	0.95	0.11	0.13	0.90	0.03
	Ssk.sd	3	6.01	0.02	1.00	0.69	0.30	0.62	0.36	0.04



364

365 Figure 3. Case study A: Diet-related differences in dental microwear, from crushing and shearing facets of upper
 366 deciduous fourth premolar of domestic pigs. Principal component analysis from the top 3 variables for each pair
 367 of dietary categories. Before the PCA, data of crushing and shearing facets have been Box-Cox transformed
 368 separately. A, bivariate graph of individuals along PC1 versus PC2; B, correlation circle, PC1 versus PC2.

369 **Case study B: Meta-analysis of a large multi-species sample**

370 The analysis, a rank by post-hoc (mean) classification performed on crushing facets after
 371 Box-Cox transformation (Table 5), revealed that the most discriminant variables were a mix of
 372 central and heterogeneity variables. After removing variables correlated with the best ranked
 373 variables, the majority of variables are heterogeneity variables related to the highest
 374 percentiles among subsampled tiles (Sh.lst.05, Asfc2.max.05, Smc2.lst.25, s.sl.lst.05,
 375 b.sl.max.05 and Sku.lst.25).

376 The major influence of the highest percentile variables is confirmed by the PCA (Fig. 4).
 377 Indeed, these variables contribute significantly to the first and second components, which
 378 explain 42.8 % and 22.6 % of the variance, respectively (Fig. 4B). This is also consistent with
 379 the difference in absolute surface height, which is clear on the maps: along the first

380 component, the highest value has a height amplitude of 10.95 μm (Fig. 4C, 4D) while the
381 lowest value has a height amplitude of 0.71 μm (Fig. 4C, 4E).

382 The bivariate graph of individuals for components 1 and 2, as well as the boxplot of
383 component 1, show that there is a large overlap between categories, both at the species and
384 the tribe level (Fig. 4A, 4C). This is due to the broad dispersion of values. When comparing
385 the means between species (Fig. 4C), the most folivorous species (*Trachypithecus auratus*,
386 *Colobus guereza* and *Ptilocolobus badius*) have the lowest PC1 values. They are followed by
387 terrestrial graminivorous papionines *Papio hamadryas* and *Theropithecus gelada*, then
388 *Nasalis larvatus*, *Semnopithecus entellus* and *Trachypithecus cristatus*. The three latter are
389 also folivorous but present higher *Asfc2* values in our sample, indicating the opportunistic
390 consumption of seeds (Thiery et al., 2021). This is supported by the surprisingly large breadth
391 of PC1 value dispersion for these three species, especially *T. cristatus*. Then, opportunistic
392 terrestrial cercopithecines and papionines show higher PC1 values, with the highest values
393 found in the hard seed predator *Lophocebus albigena* (Lambert et al., 2004) and *Macaca*
394 *sylvanus*, one of the most granivorous macaque (Kato et al., 2014).

395

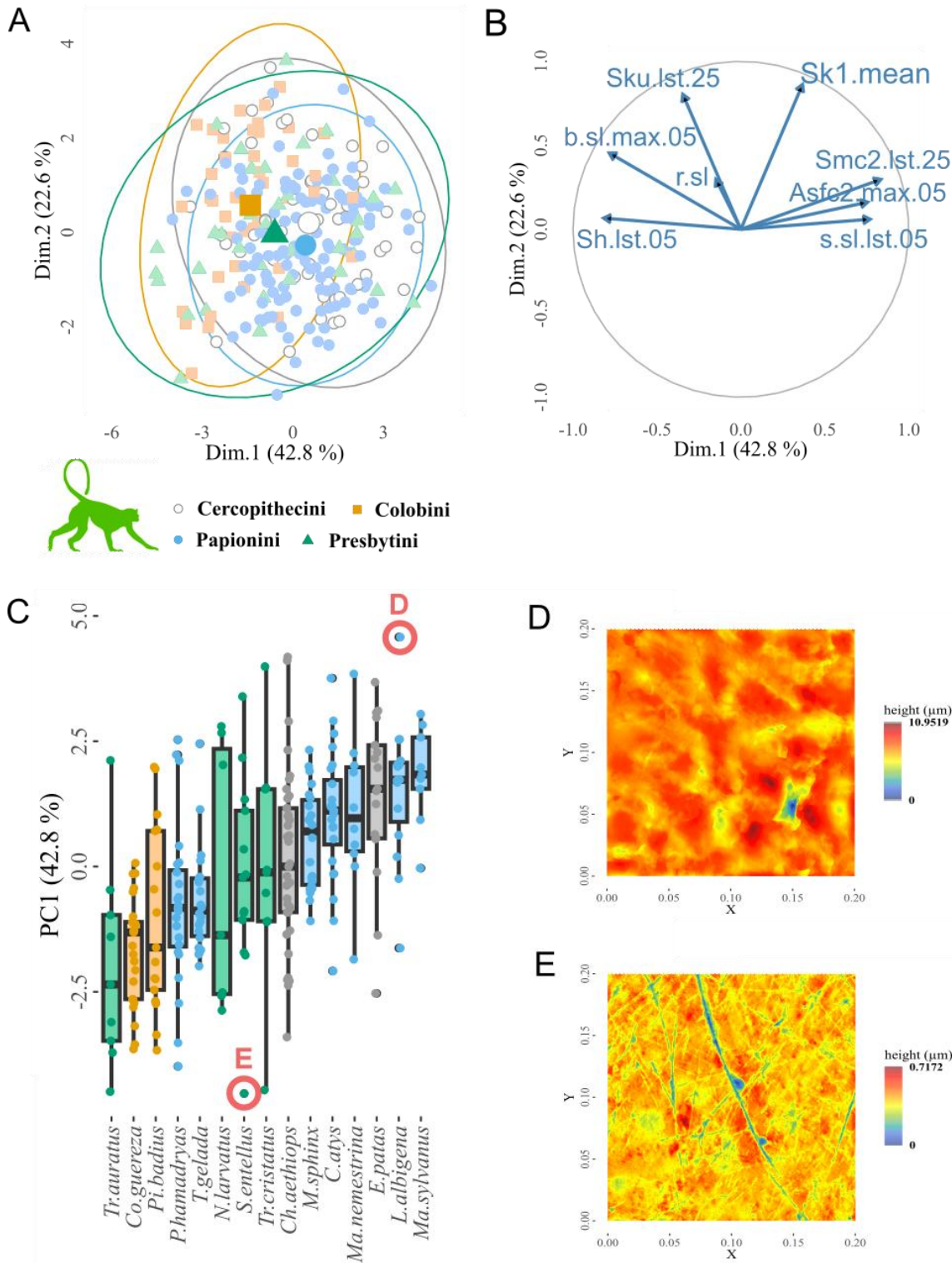
396
397

Table 5. Case study B; Meta-analysis of a large multi-species sample, the most discriminant variables for each family, classified by the number of pair (N) that shows significant differences with the Tukey's HSD p-value.

Variable	Position	ANOVA		Tukey's HSD		
		F	p value	mean p-value	geometric mean p-value	N
Sh.lst.05	1	11.29	<0.01	0.01	<0.01	37
Asfc2.max.05	5	7.62	<0.01	0.01	<0.01	32
Sp.max.25	12	9.48	<0.01	0.01	0.01	24
Sa	13	9.39	<0.01	0.01	<0.01	23
Sq	15	9.03	<0.01	0.01	0.01	23
Sv.fst.05	16	6.11	<0.01	0.01	0.01	23
Sdar.max.05	18	6.37	<0.01	0.01	<0.01	22
Smd.max.25	25	5.84	<0.01	0.01	<0.01	17
Smc2.lst.25	29	6.58	<0.01	0.01	<0.01	15
Smc1.min.25	30	5.73	<0.01	0.02	<0.01	15
Sk2.mean	33	4.51	<0.01	0.02	0.01	15
Sm.min.25	36	6.41	<0.01	0.02	0.01	14
s.sl.lst.05	45	4.71	<0.01	0.02	0.02	13
b.sl.max.05	49	6.37	<0.01	0.01	<0.01	12
Snb2.mean	60	3.53	<0.01	0.02	0.01	12
Sal.min.05	73	5.85	<0.01	0.01	<0.01	10
Sku.lst.25	83	3.42	<0.01	0.01	<0.01	9
Sk1.mean	92	4.72	<0.01	0.03	0.02	9
r.sl	99	4.88	<0.01	0.01	<0.01	7
Stri	101	4.89	<0.01	0.01	<0.01	7
Ssk.fst.05	103	4.08	<0.01	0.02	0.01	7
Snb1.sd	149	3.30	<0.01	0.02	0.01	4

398
399
400
401

All variables Box-Cox transformed. For each parameter (e.g., Sh), only the variable with the best positioning was selected (e.g., Sh.lst.05). Highlighted in grey are the best-positioned variables which are little correlated to each other (threshold: 0.7).



402
 403 Figure 4. Case study B: Meta-analysis of a large multi-species sample. Analysis of dental microwear textures
 404 from the crushing facets of upper and lower molars of cercopithecids from Asia and Africa. Principal component
 405 analysis was performed using the best-ranked non-correlated variables. Before PCA, data were Box-Cox
 406 transformed. A, bivariate graph of individuals along PC1 versus PC2; B, correlation circle, PC1 versus PC2; C,
 407 Boxplot of PC1 values, ordered by ascending mean, with species as factor. Colors indicate the tribe (blue,
 408 papionines; green, presbytines; grey, cercopithecines; orange, colobines); D, height map of the surface from the
 409 individual with the highest PC1 value (*L.albigena*_NHMB-LP-2908); E, height map of the surface from the
 410 individual with the lowest PC1 value (*S.entellus*_BM30-11-1-4). Ellipses depict the confidence interval at 95 %.

411 **Case study C: Comparison with extant species to infer the diet of extinct species**

412 The first part of the analysis, a rank by post-hoc (mean) classification performed, after a base-
413 10 log transformation, on the shearing dental facets of molars of the wild-caught ruminants
414 from the Bauges Natural Regional Park (Table 6), revealed once again that most discriminant
415 variables were a mix of central and heterogeneity variables. After removing variables
416 correlated with the best-ranked variables, what remains are variables based on spatial
417 parameters (Rmax.min.25, s.sl.mean, r.sl), the standard deviation of topology parameters
418 (Sk1.sd, Smc1.sd) and Sm.fst.25, which is the first quartile of the lowest parts of the surface's
419 height.

420 The first two dimensions of the PCA encompass 43.9 % and 27.6 % of the variance,
421 respectively. On the first dimension, we found that *G. torticornis* significantly differed from both
422 *C. capreolus* and *C. elaphus* (Table 7). In contrast, there was no significant difference
423 between *G. torticornis*, *R. rupicapra* and *O. gmelini*, which is visible on the bivariate graph and
424 on the boxplot (Fig. 5C, D). On the second dimension as well on the third and fourth
425 dimensions, *G. torticornis* was significantly different from all extant species whereas no
426 difference could be detected between extant species. Overall, *G. torticornis* had on average
427 lower values than extant species for both first and second dimensions (Fig. 5D, E).

428

429

430
431
432

Table 6. Case study C: Comparison with extant species to infer the diet of extinct species, the most discriminant variables for each parameter, classified by the number of groups significantly discriminated using Tukey's HSD p-value.

Variable	rank	F	ANOVA	p value		Number of significant differences
				HSD arithmetic mean	HSD geometric mean	
Rmax.min.25	1	7.93	<0.01	0.02	0.01	4
Snb1.sd	2	9.19	<0.01	0.01	<0.01	3
Sku.lst.25	12	6.38	<0.01	0.01	<0.01	2
Sk1.sd	13	4.38	0.01	0.01	0.01	2
Ssk.max.05	14	5.08	<0.01	0.02	0.01	2
b.sl.min.25	21	5.10	<0.01	0.02	0.01	2
Sm.fst.25	27	3.65	0.02	0.03	0.02	2
s.sl.mean	30	5.49	<0.01	0.03	0.03	2
Smd.min.05	32	3.36	0.03	0.03	0.03	2
Smc1.sd	36	4.27	0.01	0.03	0.03	2
Snb2.sd	49	5.22	<0.01	<0.01	<0.01	1
Sal	55	4.26	0.01	0.02	0.02	1
r.sl	63	3.00	0.04	0.03	0.03	1
Sa.lst.25	70	3.45	0.02	0.04	0.04	1
Stri	72	2.27	0.09	0.04	0.04	1

433
434
435
436

All data log-transformed (base 10). For each parameter (e.g., Rmax), only the variable with the best positioning was selected (e.g., Rmax.min.25). Highlighted in grey are the best positioned variables which are little correlated to each others (threshold: 0.7).

437

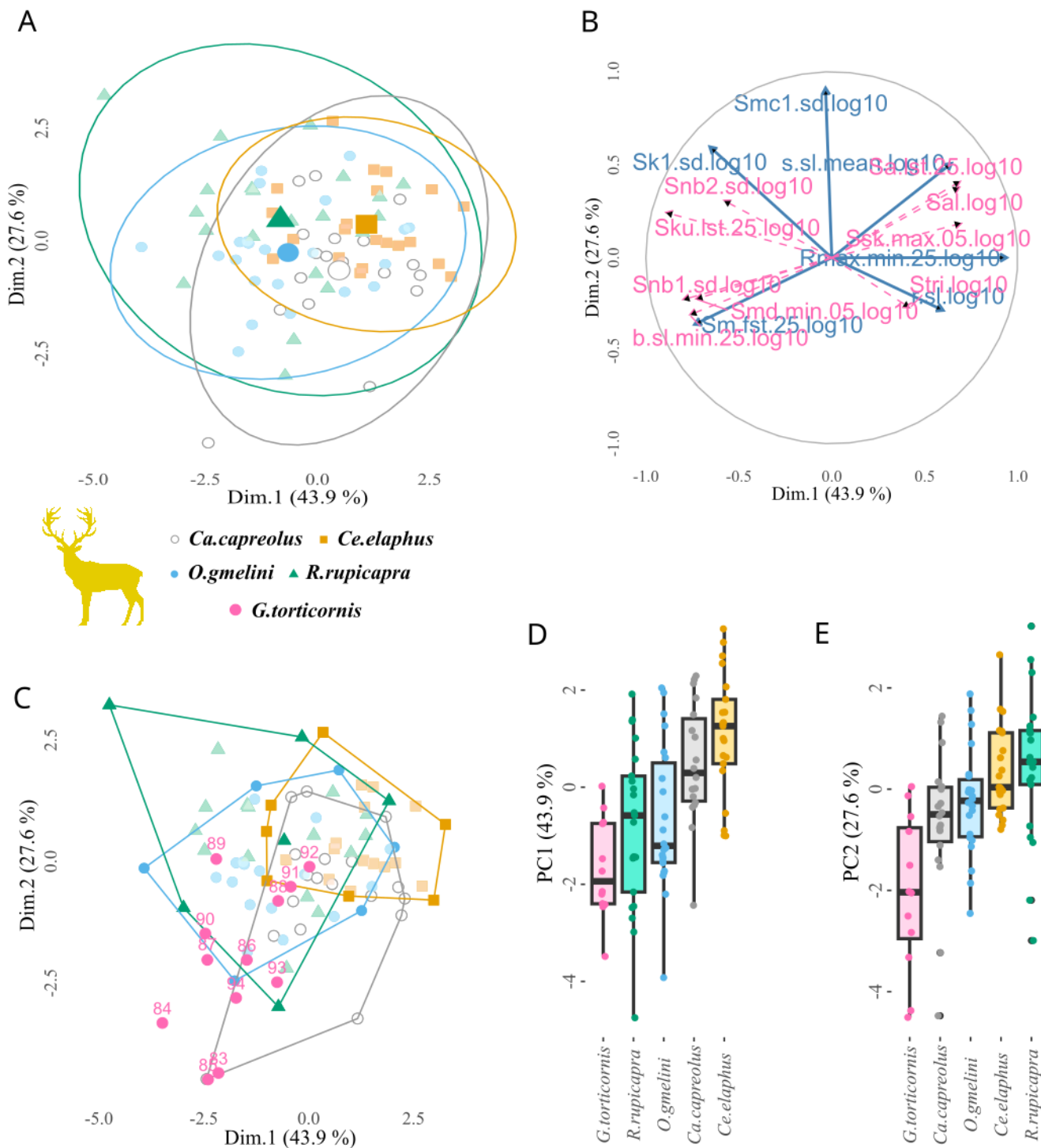
438

439

440 Table 7. Case study C: Comparison between extant and extinct species to infer the diet of the extinct species
 441 thanks to ANOVA on the first four principal components and followed by pairwise comparison of the means using
 442 Tukey's HSD.

Pair	PC1 (43.9 %)		PC2 (27.6 %)		PC3 (14.6 %)		PC4 (7.9 %)	
	Difference	p adjusted	Difference	p adjusted	Difference	p adjusted	Difference	p adjusted
CE-CC	0.61	0.66	1.02	0.10	-0.01	1.00	0.15	0.97
OG-CC	-1.14	0.09	0.39	0.87	-0.40	0.64	0.06	1.00
RR-CC	-1.31	0.04	1.12	0.06	0.28	0.87	0.15	0.96
OG-CE	-1.75	<0.01	-0.63	0.50	-0.39	0.63	-0.09	0.99
RR-CE	-1.92	<0.01	0.10	1.00	0.29	0.84	0.00	1.00
RR-OG	-0.17	0.99	0.73	0.34	0.68	0.11	0.09	0.99
GT-CC	-2.17	<0.01	-1.39	0.03	-1.54	<0.01	-1.97	<0.01
GT-CE	-2.78	<0.01	-2.41	<0.01	-1.53	<0.01	-2.12	<0.01
GT-OG	1.03	0.25	1.79	<0.01	1.14	0.01	2.03	<0.01
GT-RR	0.86	0.44	2.52	<0.01	1.82	<0.01	2.12	<0.01

443 Highlighted in grey are the differences supported by a significant adjusted p value. CE, *Cervus elaphus*; CC,
 444 *Capreolus capreolus*; GT, *Gazellospira torticornis*; OG, *Ovis gmelini*; RR, *Rupicapra rupicapra*.
 445



446
447
448
449
450
451
452
453
454

Figure 5. Case study C: Comparison with extant species to infer the diet of extinct species, PCA on selected variables with ruminants from the Bauges as individuals and fossil specimens of *Gazellospira torticornis* as supplementary individuals. A, Bivariate graph on extant specimens, PC1 versus PC2; B, Correlation circle with non-selected variables as supplementary variables (pink dashed lines), PC1 versus PC2; C, Bivariate graph of individuals along PC1 versus PC2, with the extinct species from Dafnero *Gazellospira torticornis* as supplementary individuals (pink); D, Boxplot of PC1 values, ordered by ascending mean, with species as factor; E, Boxplot of PC2 values, ordered by ascending mean, with species as factor. All data log-transformed (base 10). Ellipses depict the confidence interval at 95 %.

455 **Discussion**

456 **Case study A: Diet-related differences in dental microwear**

457 The broad spectrum of analytic tools and exploratory methods offered by trident maximizes
458 the potential for detecting diet-related differences in dental microwear. In case study A, the
459 four groups could be separated, which is consistent with Louail et al. (2021), but the
460 difference between categories was enhanced. Dental microwear sometimes shows large
461 within-species differences, including in wild animals (Calandra & Merceron, 2016, Percher et
462 al., 2018) and extinct species (Scott et al., 2005; Thiery et al., 2021). In our case study
463 however, even the subtlest variations in diet, for instance between the corn silage and the
464 control groups, could be detected. These results are promising for paleontological and
465 archaeological studies interested in diet variation across time and space.

466 In addition, trident is also compatible with other workflows, as it can easily combine multiple
467 datasets, for instances microwear measured using different methods (SSFA, light
468 microscopy...), from different teeth, or from different parts of a tooth – as in case study A. In
469 this case study, we found that shearing and crushing facets not only differ in microwear
470 textures, but also in the best ranked variables diet-wise. Crushing different kinds of food
471 influenced the skewness and heterogeneity of microwear height, whereas shearing different
472 kinds of foods had a more visible influence on height kurtosis, on standard deviation of height
473 skewness, on median height, as well as skewness and kurtosis of spatial parameters. For
474 crushing, the presence of large and deep pits resulting from the processing of hard, seed-like
475 foods is indeed expected to affect height and its heterogeneity. For shearing on the other
476 hand, spatial parameters, and especially anisotropy, are expected to be more affected by the
477 long shearing motions of tough, high-energy release rate foods such as leaves, grass etc.
478 This is consistent with our results, and demonstrates that trident can not only integrate
479 multiple methods, but also leverage their input.

480 **Case study B: Meta-analysis of a large multi-species sample**

481 Sometimes the objective is not to separate groups of individuals, but to identify patterns of
482 variation imputable to dietary trends. This is exactly what trident enabled in case study B:
483 despite PC1 values overlapping between cercopithecoid species, we can distinguish a
484 continuum from strict leaf consumption to staple seed predation (Fig. 4). The most folivorous
485 species (*Trachypithecus auratus*, *Colobus guereza* and *Ptilocolobus badius*) have the lowest
486 PC1 values, whereas opportunistic terrestrial cercopithecines and papionines show higher
487 PC1 values, with the highest values found in *Lophocebus albigena* and *Macaca sylvanus*, two
488 notable seed eaters (Lambert et al., 2004; Kato et al., 2014). Detecting this pattern required
489 trident for ranking variables by mean p-value of Tukey's HSD and for performing multivariate
490 analysis on the best non-correlated variables, but also the R environment for ordering
491 species-related boxplots by ascending mean (Fig. 4C). It shows the interest of nesting trident
492 within the R environment: accessing a broad range of libraries for complementing and
493 leveraging functions from the R package trident.

494 trident also allows to inspect surfaces using 2D and 3D maps – although these functions are
495 not implemented into the interface, they can be launched from R (see Supplementary
496 Materials 2). Here, the highest PC1 values are characterized by high maximal complexity, but
497 also deeply worn surfaces (Fig. 4D). In contrast, the lowest PC1 values are characterized by
498 a low complexity and shallow wear marks (Fig. 4E). Both a higher complexity (Ramdarshan et
499 al., 2016) and larger, deeper pits (Teaford, 1985, 1988) have been associated to the ingestion
500 of large amounts of seed kernels, which is consistent with the pattern observed on Fig. 4C. It
501 is also consistent with Asfc2 successfully separating seed-eating cercopithecoids in previous
502 studies (e.g., Thiery et al., 2021). In short, trident helps detect patterns in dental microwear
503 textures, but it also and foremost helps interpret them in biomechanical or ecological terms.

504 **Case study C: Comparison with extant species to infer the diet of extinct species**

505 The last key use of trident is inference of diet, either in extant or in extinct species. In case
506 study C, we could infer the diet of *Gazellospira torticornis*, an extinct antelope from the Early
507 Pleistocene of Greece (Hermier *et al.*, 2020). To do so, we used trident to perform a PCA on
508 the best ranked, non-correlated variables regarding their ability to separate four ruminants
509 from the Bauges Natural Regional Park with known differences in diet, ranging from selective
510 browsing to grass-dominated mixed feeding habits. We then added *G. torticornis* specimens
511 as supplementary individuals to the PCA. This analysis showed that *G. torticornis* had low
512 values of anisotropy, especially the 1st quartile (Rmax.min.25, Fig. 5), which is similar to *Ovis*
513 *gmelini* and *Rupicapra rupicapra*. Both are mixed-feeding species: *O. gmelini musimon* eats
514 grasses in complement with dicots foliages, shrubs and herbaceous dicots (Redjadj *et al.*
515 2014; see also Marchand *et al.*, 2013), while *R. rupicapra* alternates between grass and
516 foliage depending on seasons (Redjadj *et al.* 2014; see also Pérez-Barberia *et al.*, 1997). *G.*
517 *torticornis* likely was a mixed feeding species, incorporating both grasses and lignified tissues
518 in its diet.

519 Once again, nesting trident in the R environment gives access to a broad range of methods
520 for complementary analysis. To better understand the dietary behavior of *G. torticornis*, we
521 performed an ANOVA on principal components to search for differences between extinct and
522 extant taxa. For PC1, *G. torticornis* significantly differed from *Cervus elaphus* and *Capreolus*
523 *capreolus*. *C. elaphus* is also a mixed-feeding species (Gebert & Verheyden-Tixier, 2001), but
524 in the Bauges Natural Regional Park, its diet comprises a large proportion of grasses
525 (Merceron, Berlioz, *et al.*, 2021). This likely increased its dental microwear anisotropy, which
526 explains why it differs from other mixed-feeders that include more lignified tissues than the
527 red deer. *C. capreolus* on the other hand is a selective browser (Redjadj *et al.*, 2014).

528 Lastly, variables that contribute to PC2 (Smc1.sd and to some extent, Sk1.sd and s.sl.mean)
529 were significantly lower in *G. torticornis* compared to all four extant species. This point
530 illustrates how dental microwear textures can present original patterns in the fossil record,
531 sometimes completely different to what is known for extant species – perhaps reflecting how
532 different the environmental conditions were at the time.

533 **Conclusion**

534 trident, an R package for performing dental microwear texture analysis is here proposed and
535 shown with three case studies, showing how trident helps answer questions commonly
536 investigated by paleontologists and archaeologists. In the first case study, we separate four
537 groups of domestic pigs based on their dietary composition. In the second case study, we
538 identify microwear texture patterns in a large database of 15 primate species and relate these
539 patterns to biomechanical and ecological factors. The third case study investigates the dental
540 microwear textures of four extant ruminants to infer the diet of an extinct antelope from the
541 Pleistocene of Greece. These case studies show how trident can leverage dental microwear
542 texture analysis results.

543 **Acknowledgments**

544 This study was funded by the French National Agency for Research (ANR-13-JSV7-0008-01
545 Trident, PI: Gildas Merceron; ANR-17-CE27-0002-02 DIET-Scratches, PIs: Gildas Merceron,
546 Stéphane Ferchaud) and the Region of Nouvelle Aquitaine (ALIHOM #210389; PI: Gildas
547 Merceron). We thank all the people who helped improve trident during its development, and
548 especially Anusha Ramdarshan, Antoine Souron and Franck Guy. Our gratitude also goes
549 towards the colleagues who allowed or participated in data collection for the three case
550 studies, notably Jérôme Surault (PALEVOPRIM).

551 **Authors' contributions**

552 AF, NB, and GM conceived the ideas and designed the methodology; GM, CB, ML, AW and
553 EB collected the data; GT, ML and GM analyzed the data; AF, GT and GM developed the
554 software; GM acquired funding and managed the project administration. All authors
555 contributed critically to the drafts and gave final approval for publication.

556 **Data availability**

557 The source package is available on Github at <https://github.com/nialsiG/trident>.

- Calandra, I., & Merceron, G. (2016). Dental microwear texture analysis in mammalian ecology: DMTA in ecology. *Mammal Review*, *46*(3), 215–228. <https://doi.org/10.1111/mam.12063>
- Francisco, A., Blondel, C., Brunetière, N., Ramdarshan, A., & Merceron, G. (2018a). Enamel surface topography analysis for diet discrimination. A methodology to enhance and select discriminative parameters. *Surface Topography: Metrology and Properties*, *6*(1), 015002. <https://doi.org/10.1088/2051-672X/aa9dd3>
- Francisco, A., Brunetière, N., & Merceron, G. (2018b). Gathering and Analyzing Surface Parameters for Diet Identification Purposes. *Technologies*, *6*(3), 75. <https://doi.org/10.3390/technologies6030075>
- Galbany, J., Martínez, L. M., López-Amor, H. M., Espurz, V., Hiraldo, O., Romero, A., de Juan, J., & Pérez-Pérez, A. (2005). Error rates in buccal-dental microwear quantification using scanning electron microscopy. *Scanning*, *27*(1), 23–29. <https://doi.org/10.1002/sca.4950270105>
- Gebert, C., & Verheyden-Tixier, H. (2001). Variations of diet composition of Red Deer (*Cervus elaphus* L.) in Europe. *Mammal Review*, *31*(3–4), 189–201. <https://doi.org/10.1111/j.1365-2907.2001.00090.x>
- Gordon, K. D. (1982). A study of microwear on chimpanzee molars: Implications for dental microwear analysis. *American Journal of Physical Anthropology*, *59*(2), 195–215. <https://doi.org/10.1002/ajpa.1330590208>
- Grine, F. E., Ungar, P. S., & Teaford, M. F. (2002). Error rates in dental microwear quantification using scanning electron microscopy. *Scanning*, *24*(3), 144–153. <https://doi.org/10.1002/sca.4950240307>
- Hermier, R., Merceron, G., & Kostopoulos, D. S. (2020). The emblematic Eurasian Villafranchian antelope *Gazellospira* (Mammalia: Bovidae): New insights from the Lower Pleistocene Dafnero fossil sites (Northern Greece). *Geobios*, *61*, 11–29.
- Hua, L., Chen, J., & Ungar, P. S. (2020). Diet reduces the effect of exogenous grit on tooth microwear. *Biosurface and Biotribology*, *6*(2), 48–52. <https://doi.org/10.1049/bsbt.2019.0041>

- Kaiser, T. M., Clauss, M., & Schulz-Kornas, E. (2015). A set of hypotheses on tribology of mammalian herbivore teeth. *Surface Topography: Metrology and Properties*, 4(1), 014003.
<https://doi.org/10.1088/2051-672X/4/1/014003>
- Kato, A., Tang, N., Borries, C., Papakyrikos, A. M., Hinde, K., Miller, E., Kunimatsu, Y., Hirasaki, E., Shimizu, D., & Smith, T. M. (2014). Intra- and interspecific variation in macaque molar enamel thickness. *American Journal of Physical Anthropology*, 155(3), 447–459.
<https://doi.org/10.1002/ajpa.22593>
- Kay, R. F. (1981). The ontogeny of premolar dental wear in *Cercocebus albigena* (cercopithecidae). *American Journal of Physical Anthropology*, 54(1), 153–155.
<https://doi.org/10.1002/ajpa.1330540119>
- Lambert, J. E., Chapman, C. A., Wrangham, R. W., & Conklin-Brittain, N. L. (2004). Hardness of cercopithecine foods: Implications for the critical function of enamel thickness in exploiting fallback foods. *American Journal of Physical Anthropology*, 125(4), 363–368.
<https://doi.org/10.1002/ajpa.10403>
- Louail, M., Ferchaud, S., Souron, A., Walker, A. E. C., & Merceron, G. (2021). Dental microwear textures differ in pigs with overall similar diets but fed with different seeds. *Palaeogeography, Palaeoclimatology, Palaeoecology*, 572, 110415. <https://doi.org/10.1016/j.palaeo.2021.110415>
- Lucas, P. W., Omar, R., Al-Fadhlah, K., Almusallam, A. S., Henry, A. G., Michael, S., Thai, L. A., Watzke, J., Strait, D. S., & Atkins, A. G. (2013). Mechanisms and causes of wear in tooth enamel: Implications for hominin diets. *Journal of The Royal Society Interface*, 10(80), 20120923. <https://doi.org/10.1098/rsif.2012.0923>
- Marchand, P., Redjadj, C., Garel, M., Cugnasse, J.-M., Maillard, D., & Loison, A. (2013). Are mouflon *Ovis gmelini musimon* really grazers? A review of variation in diet composition. *Mammal Review*, 43(4), 275–291. <https://doi.org/10.1111/mam.12000>
- Merceron, G., Berlioz, E., Vohnof, H., Green, D., Garel, M., & Tütken, T. (2021). Tooth tales told by dental diet proxies: An alpine community of sympatric ruminants as a model to decipher the ecology of fossil fauna. *Palaeogeography, Palaeoclimatology, Palaeoecology*, 562, 110077.

- Merceron, G., Blondel, C., Bonis, L. D., Koufos, G. D., & Viriot, L. (2005). A New Method of Dental Microwear Analysis: Application to Extant Primates and *Ouranopithecus macedoniensis* (Late Miocene of Greece). *PALAIOS*, 20(6), 551–561. <https://doi.org/10.2110/palo.2004.p04-17>
- Merceron, G., Bonis, L., Viriot, L., & Blondel, C. (2005). Dental microwear of the late Miocene bovids of northern Greece: Vallesian/Turolian environmental changes and disappearance of *Ouranopithecus macedoniensis*? *Bulletin de La Societe Geologique de France*, 176, 475–484. <https://doi.org/10.2113/176.5.475>
- Merceron, G., Kallend, A., Francisco, A., Louail, M., Martin, F., Plastiras, C.-A., Thiery, G., & Boisserie, J.-R. (2021). Further away with dental microwear analysis: Food resource partitioning among Plio-Pleistocene monkeys from the Shungura Formation, Ethiopia. *Palaeogeography, Palaeoclimatology, Palaeoecology*, 572, 110414. <https://doi.org/10.1016/j.palaeo.2021.110414>
- Merceron, G., Ramdarshan, A., Blondel, C., Boisserie, J.-R., Brunetiere, N., Francisco, A., Gautier, D., Milhet, X., Novello, A., & Pret, D. (2016). Untangling the environmental from the dietary: Dust does not matter. *Proceedings of the Royal Society B: Biological Sciences*, 283(1838), 20161032. <https://doi.org/10.1098/rspb.2016.1032>
- Mihlbachler, M. C., Beatty, B. L., Caldera-Siu, A., Chan, D., & Lee, R. (2012). Error rates and observer bias in dental microwear analysis using light microscopy. *Palaeontologia Electronica*, 15(1), 1–22. <https://doi.org/10.26879/298>
- Percher, A.M., Merceron, G., Nsi Akoue, G., Galbany, J., Romero, A., & Charpentier, M.J. (2018). Dental microwear textural analysis as an analytical tool to depict individual traits and reconstruct the diet of a primate. *American Journal of Physical Anthropology*, 165, 123–138. <https://doi.org/10.1002/ajpa.23337>
- Peréz-Barberia, F. J., Oliván, M., Osoro, K., & Nores, C. (1997). Sex, seasonal and spatial differences in the diet of Cantabrian chamois *Rupicapra pyrenaica parva*. *Acta Theriologica*, 42(1), 37–46.
- Purnell, M. A., Crumpton, N., Gill, P. G., Jones, G., & Rayfield, E. J. (2013). Within-guild dietary discrimination from 3-D textural analysis of tooth microwear in insectivorous mammals. *Journal of Zoology*, 291(4), 249–257. <https://doi.org/10.1111/jzo.12068>

- Ramdarshan, A., Blondel, C., Brunetière, N., Francisco, A., Gautier, D., Surault, J., & Merceron, G. (2016). Seeds, browse, and tooth wear: A sheep perspective. *Ecology and Evolution*, 6(16), 5559–5569. <https://doi.org/10.1002/ece3.2241>
- Redjadj, C., Darmon, G., Maillard, D., Chevrier, T., Bastianelli, D., Verheyden, H., Loison, A., & Saïd, S. (2014). Intra- and Interspecific Differences in Diet Quality and Composition in a Large Herbivore Community. *PLOS ONE*, 9(2), e84756. <https://doi.org/10.1371/journal.pone.0084756>
- Rivals, F., & Semprebon, G. M. (2011). Dietary plasticity in ungulates: insight from tooth microwear analysis. *Quaternary International*, 245(2), 279–284. <https://doi:10.1016/j.quaint.2010.08.001>
- Rowe, N., Goodall, J., & Mittermeier, R. (1996). *The pictorial guide to the living primates* (Vol. 236). Pogonias Press.
- Sanson, G. D., Kerr, S. A., & Gross, K. A. (2007). Do silica phytoliths really wear mammalian teeth? *Journal of Archaeological Science*, 34(4), 526–531. <https://doi.org/10.1016/j.jas.2006.06.009>
- Schulz, E., Calandra, I., & Kaiser, T. M. (2010). Applying tribology to teeth of hoofed mammals. *Scanning*, 32(4), 162–182. <https://doi.org/10.1002/sca.20181>
- Schulz- Kornas, E., Stuhlträger, J., Clauss, M., Wittig, R. M., & Kupczik, K. (2019). Dust affects chewing efficiency and tooth wear in forest dwelling Western chimpanzees (*Pan troglodytes verus*). *American Journal of Physical Anthropology*, 169(1), 66–77. <https://doi.org/10.1002/ajpa.23808>
- Schulz-Kornas, E., Winkler, D. E., Clauss, M., Carlsson, J., Ackermans, N. L., Martin, L. F., Hummel, J., Müller, D. W. H., Hatt, J.-M., & Kaiser, T. M. (2020). Everything matters: Molar microwear texture in goats (*Capra aegagrus hircus*) fed diets of different abrasiveness. *Palaeogeography, Palaeoclimatology, Palaeoecology*, 552, 109783. <https://doi.org/10.1016/j.palaeo.2020.109783>
- Scott, R. S., Ungar, P. S., Bergstrom, T. S., Brown, C. A., Childs, B. E., Teaford, M. F., & Walker, A. (2006). Dental microwear texture analysis: Technical considerations. *Journal of Human Evolution*, 51(4), 339–349. <https://doi.org/10.1016/j.jhevol.2006.04.006>
- Scott, R. S., Ungar, P. S., Bergstrom, T. S., Brown, C. A., Grine, F. E., Teaford, M. F., & Walker, A. (2005). Dental microwear texture analysis shows within-species diet variability in fossil hominins. *Nature*, 436(7051), 693–695. <https://doi.org/10.1038/nature03822>

- Solounias, N., & Semperebon, G. (2002). Advances in the reconstruction of ungulate ecomorphology with application to early fossil equids. *American Museum Novitates*, 2002(3366), 1-49.
[https://doi.org/10.1206/0003-0082\(2002\)366<0001:AITROU>2.0.CO;2](https://doi.org/10.1206/0003-0082(2002)366<0001:AITROU>2.0.CO;2)
- Teaford, M. F. (1985). Molar microwear and diet in the genus *Cebus*. *American Journal of Physical Anthropology*, 66(4), 363–370. <https://doi.org/10.1002/ajpa.1330660403>
- Teaford, M. F. (1988). A review of dental microwear and diet in modern mammals. *Scanning Microscopy*, 2(2), 1149–1166.
- Teaford, M. F., Maas, M. C., & Simons, E. L. (1996). Dental microwear and microstructure in early oligocene primates from the Fayum, Egypt: Implications for diet. *American Journal of Physical Anthropology*, 101, 527–543.
- Teaford, M. F., & Oyen, O. J. (1989). In vivo and in vitro turnover in dental microwear. *American Journal of Physical Anthropology*, 80(4), 447–460. <https://doi.org/10.1002/ajpa.1330800405>
- Teaford, M. F., Ungar, P. S., Taylor, A. B., Ross, C. F., & Vinyard, C. J. (2020). The dental microwear of hard- object feeding in laboratory *Sapajus apella* and its implications for dental microwear formation. *American Journal of Physical Anthropology*, 171(3), 439–455.
<https://doi.org/10.1002/ajpa.24000>
- Thierry, G., Gibert, C., Guy, F., Lazzari, V., Geraads, D., Spassov, N., & Merceron, G. (2021). From leaves to seeds? The dietary shift in late Miocene colobine monkeys of southeastern Europe. *Evolution*, 75(8), 1983–1997. <https://doi.org/10.1111/evo.14283>
- Ungar, P. S. (1996). Dental microwear of European Miocene catarrhines: Evidence for diets and tooth use. *Journal of Human Evolution*, 31(4), 335–366. <https://doi.org/10.1006/jhev.1996.0065>
- Ungar, P. S., Brown, C. A., Bergstrom, T. S., & Walker, A. (2003). Quantification of dental microwear by tandem scanning confocal microscopy and scale-sensitive fractal analyses. *Scanning*, 25(4), 185–193. <https://doi.org/10.1002/sca.4950250405>
- Ungar, P. S., Grine, F. E., & Teaford, M. F. (2008). Dental Microwear and Diet of the Plio-Pleistocene Hominin *Paranthropus boisei*. *PLOS ONE*, 3(4), e2044.
<https://doi.org/10.1371/journal.pone.0002044>

- Walker, A., Hoeck, H. N., & Perez, L. (1978). Microwear of Mammalian Teeth as an Indicator of Diet. *Science*, 201(4359), 908–910. <https://doi.org/10.1126/science.684415>
- Weber, K., Winkler, D. E., Kaiser, T. M., Žigaitė, Ž., & Tütken, T. (2021). Dental microwear texture analysis on extant and extinct sharks: Ante- or post-mortem tooth wear? *Palaeogeography, Palaeoclimatology, Palaeoecology*, 562, 110147. <https://doi.org/10.1016/j.palaeo.2020.110147>
- Wickham, H., Chang, W., Henry, L., Pedersen, T. L., Takahashi, K., Wilke, C., Woo, K., Yutani, H., Dunnington, D., & RStudio. (2021). *ggplot2: Create Elegant Data Visualisations Using the Grammar of Graphics* (3.3.5) [Computer software]. <https://CRAN.R-project.org/package=ggplot2>
- Williams, V. S., Barrett, P. M., & Purnell, M. A. (2009). Quantitative analysis of dental microwear in hadrosaurid dinosaurs, and the implications for hypotheses of jaw mechanics and feeding. *Proceedings of the National Academy of Sciences*, 106(27), 11194–11199. <https://doi.org/10.1073/pnas.0812631106>
- Winkler, D. E., Schulz-Kornas, E., Kaiser, T. M., Codron, D., Leichliter, J., Hummel, J., Martin, L. F., Clauss, M., & Tütken, T. (2020). The turnover of dental microwear texture: Testing the “last supper” effect in small mammals in a controlled feeding experiment. *Palaeogeography, Palaeoclimatology, Palaeoecology*, 557, 109930. <https://doi.org/10.1016/j.palaeo.2020.109930>
- Winkler, D. E., Schulz-Kornas, E., Kaiser, T. M., & Tütken, T. (2019). Dental microwear texture reflects dietary tendencies in extant Lepidosauria despite their limited use of oral food processing. *Proceedings of the Royal Society B: Biological Sciences*, 286(1903), 20190544. <https://doi.org/10.1098/rspb.2019.0544>